Bull. Soc. R. Sci. Liège, 2024, **93**(3), 216–229 *Peer-reviewed conference paper*
doi:10.25518/0037-9565.12319

Charting New Pathways to Form Wolf–Rayet Stars at Low Metallicities

Daniel PAULI

Institut für Physik und Astronomie, Universität Potsdam, Germany
Correspondence to: dpauli@astro.physik.uni-potsdam.de

Paper presented at the 41st Liège International Astrophysical Colloquium on "The eventful life of massive star multiples," University of Liège (Belgium), 15–19 July 2024.

Abstract

Low-metallicity Wolf–Rayet (WR) populations, such as the one of the Small Magellanic Cloud (SMC), are expected to be slightly influenced by metallicity-dependent effects, such as envelope inflation, which typically positions stars at cooler temperatures. Consequently, these populations should be easier to understand from a theoretical point of view. Yet, the observed bimodal temperature distribution of WR stars in the SMC cannot be explained by existing single-star or binary evolution models. To better understand the observed temperature distribution of WR stars in the SMC, the role of the evolutionary secondary and its response to mass transfer is studied here in detail. To achieve this, I calculated a small grid of binary evolution models at the SMC metallicity, that follows the evolution of both the primary and secondary stars in detail. The analysis of the new binary evolution models suggests that hot ($T \approx 100\,\mathrm{kK}$), hydrogen-poor WN-type stars are the descendants of "ordinary" primary stars or secondaries that have accreted less than a few percent of their initial mass. In contrast, moderate-temperature ($T \approx 50\,\mathrm{kK}$) WN stars can emerge through two channels: (i) as former accretors that underwent rejuvenation, altering their interior structure and leading to higher surface oxygen abundances ($X_\mathrm{O} = 20 \times 10^{-5}$) after mass-transfer, or (ii) as luminous stars experiencing envelope inflation, that exhibit surface oxygen abundances in accordance with the CNO-equilibrium value ($X_\mathrm{O} = 2 \times 10^{-5}$). The first observational evidence supporting this hypothesis comes from the WR star SMC AB 4, whose optical spectra can only be explained with a stellar atmosphere model having a surface oxygen abundance one order of magnitude higher than the CNO-equilibrium value. Following the binary evolution models, secondary stars that have accreted mass relatively conservatively and, thus, got rejuvenated will evolve at low metallicity into WN stars with moderate temperatures and should be accompanied by a compact object. This would imply that the WN-type star SMC AB 4 should have a so far unseen compact companion. Future spectroscopic surveys focusing on surface oxygen abundances and multiplicity among SMC WR stars are key to further understanding massive star evolution and the role of binarity in forming WR stars in low-metallicity environments.

Keywords: stars: massive, stars: Wolf–Rayet, stars: evolution, binaries: close, Magellanic Clouds

1. Introduction

Wolf-Rayet (WR) stars are massive, helium-enriched stars characterized by strong, optically thick winds that manifest themselves as broad emission lines in their stellar spectra (Castor et al., 1975; Crowther, 2007). These stars are associated with the late evolutionary stages of massive O-type stars that have lost most of their hydrogen-rich outer envelopes through powerful stellar winds, luminous blue variable (LBV) outbursts, or interactions with a binary companion (Paczyński, 1967; Conti, 1976). Stars that have lost a substantial fraction of their hydrogen (H) envelope have high surface temperatures and are positioned on the left side of the zero-age main sequence (ZAMS) on the Hertzsprung–Russell diagram (HRD).

WR stars significantly impact their surroundings through their strong winds and ionizing radiation, shaping the interstellar medium and enriching it with heavy elements (Maeder, 1983; Dray et al., 2003; Weaver et al., 1977). The extent of their influence strongly depends on their stellar parameters and evolutionary states. Furthermore, WR stars are potential progenitors of hydrogen-free and superluminous supernovae (Dessart et al., 2011; Groh et al., 2013; Inserra et al., 2013; Aguilera-Dena et al., 2020, 2022), provided they can shed their remaining H-poor layers. To fully grasp the role of WR stars in the early universe and their impact on their environments, it is crucial to understand their diverse evolutionary pathways and the resultant effects on the surrounding medium.

WR stars are classified into three subtypes based on their surface composition and evolutionary stage: WN-type stars, that exhibit strong nitrogen emission lines, reflect the increased nitrogen abundances produced via the CNO cycle in the former H-burning core. These WN stars can be either H-poor or H-free, depending on the extent of envelope stripping. Other subtypes are the WC- and WO-type stars, distinguished by their prominent carbon and oxygen emission lines, respectively, indicative of core-helium burning products being exposed at their surfaces.

In our Galaxy, most WR stars are near their Eddington limit, enabling them to drive strong stellar winds. However, this proximity to the Eddington limit also triggers the effect of envelope inflation, which leads to larger apparent radii and lower surface temperatures (Gräfener et al., 2012; Sanyal et al., 2015). At solar metallicity, WR stars across different subtypes span a wide temperature range from $T \approx 40\,\mathrm{kK}$ to $150\,\mathrm{kK}$. The effect of inflation, driven primarily by changes in the iron opacity in the star's outer layers, diminishes with decreasing metallicity. Observations of WR stars in low-metallicity environments, such as the SMC (a nearby irregular dwarf galaxy with a metallicity of $Z_{\mathrm{SMC}} = \frac{1}{7} Z_{\odot}$ harboring 12 WR stars) support this trend, as most of the observed WR stars exhibit surface temperatures around $T \approx 100,\mathrm{kK}$, placing them close to the helium zero-age main sequence (He-ZAMS) (Hainich et al., 2015; Shenar et al., 2016, 2018). However, there are a few exceptions of WR stars in the SMC that also have moderate temperatures of $T \approx 50\,\mathrm{kK}$. Namely, the luminous WR binary SMC AB 5 hosts two very massive WR stars ($M_{\mathrm{WR}} \approx 60\,M_{\odot}$; Koenigsberger et al. 2014; Shenar et al. 2016) that, due to their proximity to the Eddington limit, may also experience envelope inflation, and the faint WR stars SMC AB 2 and SMC AB 4, which cannot be explained with current stellar and binary evolution models. This unexpected bi-modal temperature distribution of the WR stars in the SMC challenges our understanding of their evolutionary history.

In this paper, I present the latest results from a small grid of state-of-the-art binary evolution models at low metallicity, discussing their implications for our understanding of the analysis of WR populations and the role of these stars in low-metallicity environments.

2. Binary Evolution Models

In this work, the Modules for Experiments in Stellar Astrophysics (MESA) code version r15140 (Paxton et al., 2011, 2013, 2015, 2018, 2019) is used to calculate the evolution of the primary and secondary stars in detail. To study the effect of binary interactions on the evolution of low-metallicity massive stars a tiny grid with the metallicity of the SMC is calculated. The grid contains models with initial donor masses of $M_{\mathrm{ini},1} = 30 M_\odot$, $45 M_\odot$, and $60 M_\odot$. The secondaries always have masses such that the system has a mass-ratio of $q = 0.85$, and initial orbital periods of $P_{\mathrm{ini}} = 5\,\mathrm{d}$, $50\,\mathrm{d}$, and $500\,\mathrm{d}$. The initial parameters are chosen such that the final binary models cover roughly the luminosity ranges of the observed WR population of the SMC.

To make the models comparable to observations of stars in the SMC, the example of Brott et al. (2011) is followed. Tailored abundances of H, He, C, N, O, Mg, Si, and Fe are used (Kurt and Dufour, 1998; Venn, 1999; Hunter et al., 2007; Trundle et al., 2007). For the remaining elements, solar-abundances (Asplund et al., 2009) are scaled down to the SMC metallicity by multiplying them by a factor of $\frac{1}{7}$. Convection is treated following the mixing length theory (Böhm-Vitense, 1958) with a mixing length coefficient of $\alpha_{\mathrm{MLT}} = 1.5$ and using the Ledoux criterion for convection. During core–hydrogen burning, it is assumed that on top of the convective core, the process of overshooting material can be modeled by a step profile of size $0.335 H_P$ (Brott et al., 2011; Schootemeijer et al., 2019). Furthermore, semiconvective mixing is considered with an efficiency parameter $\alpha_{\mathrm{sc}} = 1$ (Langer et al., 1983; Schootemeijer et al., 2019). Rotational mixing is modeled as a diffusive process accounting for dynamical and secular shear instabilities, Eddington–Sweet circulations, and, Goldreich–Schubert–Fricke instabilities (Heger et al., 2000). The efficiency parameters are chosen as $f_c = \frac{1}{30}$ and $f_\mu = 0.1$ (Brott et al., 2011). In addition, angular momentum transport via magnetic fields originating from a Taylor–Spruit dynamo are considered (Spruit, 2002). Thermohaline mixing is included with an efficiency $\alpha_{\mathrm{th}} = 1$ (Kippenhahn et al., 1980).

Mass loss via stellar winds has a severe impact on the evolution of a star. To ensure that the resulting binary evolution models are comparable to the observations, mass-loss recipes for different evolutionary stages are included as follows: Mass-loss from stellar winds of hot OB-type stars ($T > 22.5\,\mathrm{kK}$ and $X_{\mathrm{H}} > 0.7$) is modeled using the recipe of Vink et al. (2001). For cooler stars ($T < 22.5\,\mathrm{kK}$), the maximum value of Vink et al. (2001) or Nieuwenhuijzen and de Jager (1990) is used. For the WR phase ($X_{\mathrm{H}} < 0.4$) the recipe from Shenar et al. (2019, 2020) is employed. For transition phases from OB-type stars to the WR stage ($0.7 > X_{\mathrm{H}} > 0.4$), the mass-loss rates are linearly interpolated between the relations from Vink et al. (2001) and those from Shenar et al. (2019, 2020).

Interactions between the binary components encompass tidal interactions, as well as mass

transfer via Roche lobe overflow and stellar winds. Within the model calculations, tidal synchronization and circularization happen on timescales as described in Hurley et al. (2002). For simplicity and to reduce the initial free parameter space, it is assumed that the stars are initially synchronized and that the orbit is circular. To model mass-transfer the implicit "contact" scheme from MESA is employed. Mass accretion on the secondary is limited by rotation, meaning that the stellar companion can only accrete material as long as it is rotating with sub-critical rotation (i.e., when tides can spin down the star efficiently). For compact object companions, the accretion is confined by the Eddington limit, preventing them from efficiently accreting material.

The evolution of a binary component is only calculated until helium is depleted in the core to ensure numerical stability. To be able to continue the evolution, it is assumed that the primary star directly collapses into a BH without a supernova explosion (Dessart et al., 2011), meaning that the system can remain bound and that the secondary can have a mass-transfer phase onto the compact companion.

3. Results

The stellar evolution tracks of the primaries are shown in the left panel of Fig. 1. To illustrate well-populated regions in the HRD, the tracks are over-plotted by dots equally spaced in time with steps every $\Delta t = 30\,000\,\mathrm{yr}$. On the right panels of Fig. 1 the temperature distribution of the WN stars in the SMC is compared to the time the models of the primaries with different initial masses spend as WRs (i.e., $T > 30\,\mathrm{kK}$ and $X_\mathrm{H} < 0.65$). It becomes evident that, independent of their initial period, all primaries with initial masses of $30\,M_\odot$ and $45\,M_\odot$ will evolve into hydrogen-poor ($X_\mathrm{H} \approx 0.2$) WN-type stars with high temperatures of about 100 kK. This agrees well with the observed hot WN-type stars in the SMC. For primaries with initial masses of $60\,M_\odot$, the effect of envelope inflation during the main sequence evolution becomes apparent, meaning that they increase in size and fill their Roche lobe earlier compared to a non-inflated star. This is also reflected in their post-interaction products, which are puffed-up hydrogen-poor ($X_\mathrm{H} \approx 0.2$ to 0.3) WN-type stars that populate the full temperature range ($T = 40$ to 100 kK) of observed WN-type stars in this luminosity regime ($\log(L/L_\odot) \gtrsim 6.1$). Note here that the primary models fail to account for the less luminous WN stars SMC AB 2 and SMC AB 4 which exhibit moderate temperatures of about 50 kK and surface hydrogen abundances between 0.2 and 0.4.

Within the model calculations, the evolution of the secondary is followed in detail. The corresponding tracks are illustrated in Fig. 2. Already on first inspection, one can notice that the evolution of a secondary is more complicated than the evolution of the primary stars. Some of these models evolve into hot, hydrogen-poor WN stars, similar to the primaries, while others end up with moderate temperatures of about 50 kK and surface hydrogen abundances around 0.4. From an analysis of the binary evolution models, I noticed that the different outcomes depend on the efficiency of mass transfer. In the binary evolution calculations presented here, accretion is limited by rotation. In the systems with orbital periods on the order of days (here, $P_\mathrm{ini} = 5\,\mathrm{d}$) the secondary can be efficiently spun down via tides, meaning that in these systems,

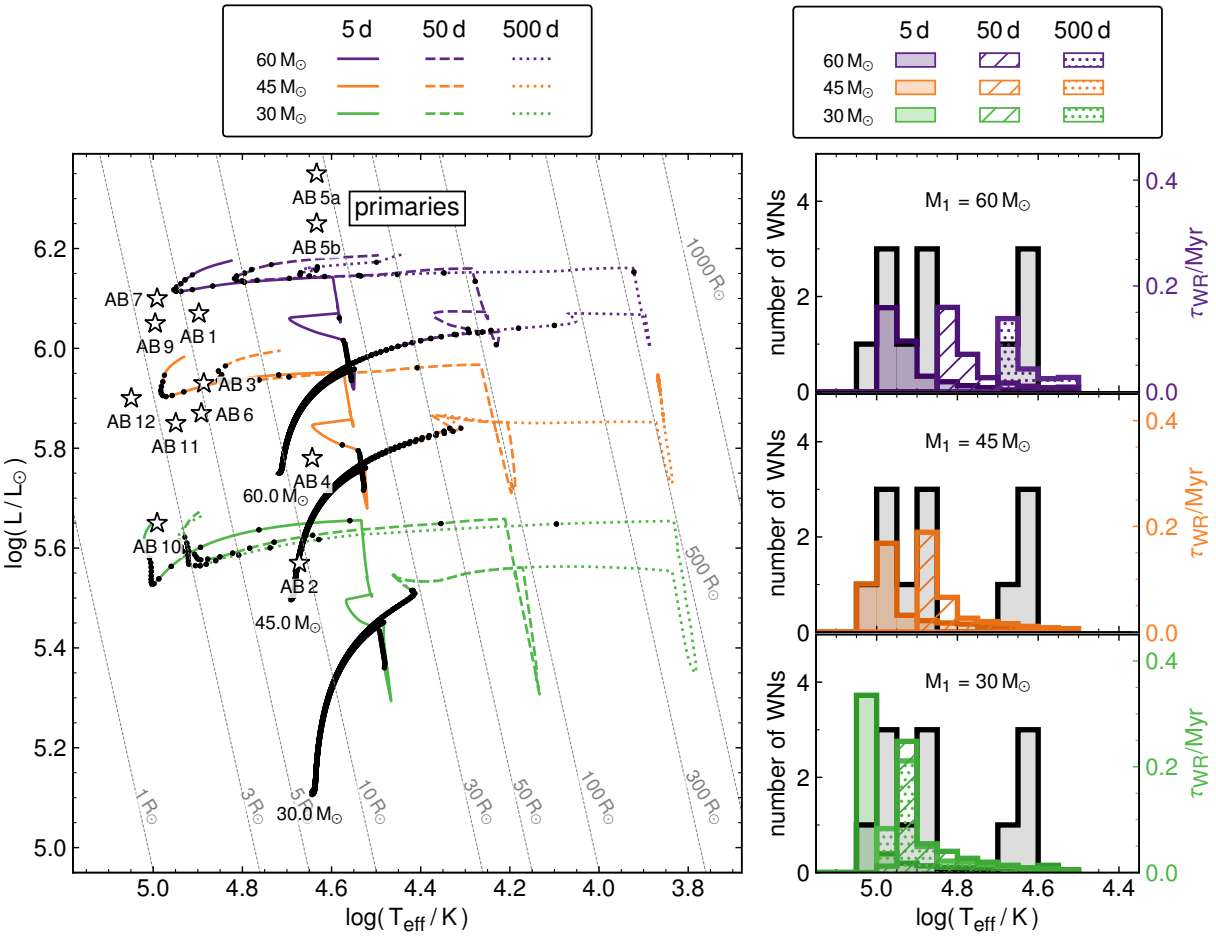

Figure 1: (*Left*) HR diagram showing stellar evolution tracks for the primary stars of the binary evolution grid. Tracks are color-coded by initial mass: green for $30\,M_\odot$, orange for $45\,M_\odot$, and purple for $60\,M_\odot$. Solid, dashed, and dotted lines represent initial orbital periods of 5 d, 50 d, and 500 d, respectively. The tracks are overplotted by black dots representing equidistant time steps of $\Delta t = 30\,000$ yr and, thus, highlighting well-populated regions. Observed WN-type stars in the SMC are marked by open star symbols and labeled by their name. (*Right panels*) Histograms comparing the temperature distribution of SMC WN-type stars (gray) with the time the primary star models spend in each temperature bin. Colored, dashed, and dotted histograms correspond to models with initial orbital periods of 5 d, 50 d, and 500 d, respectively.

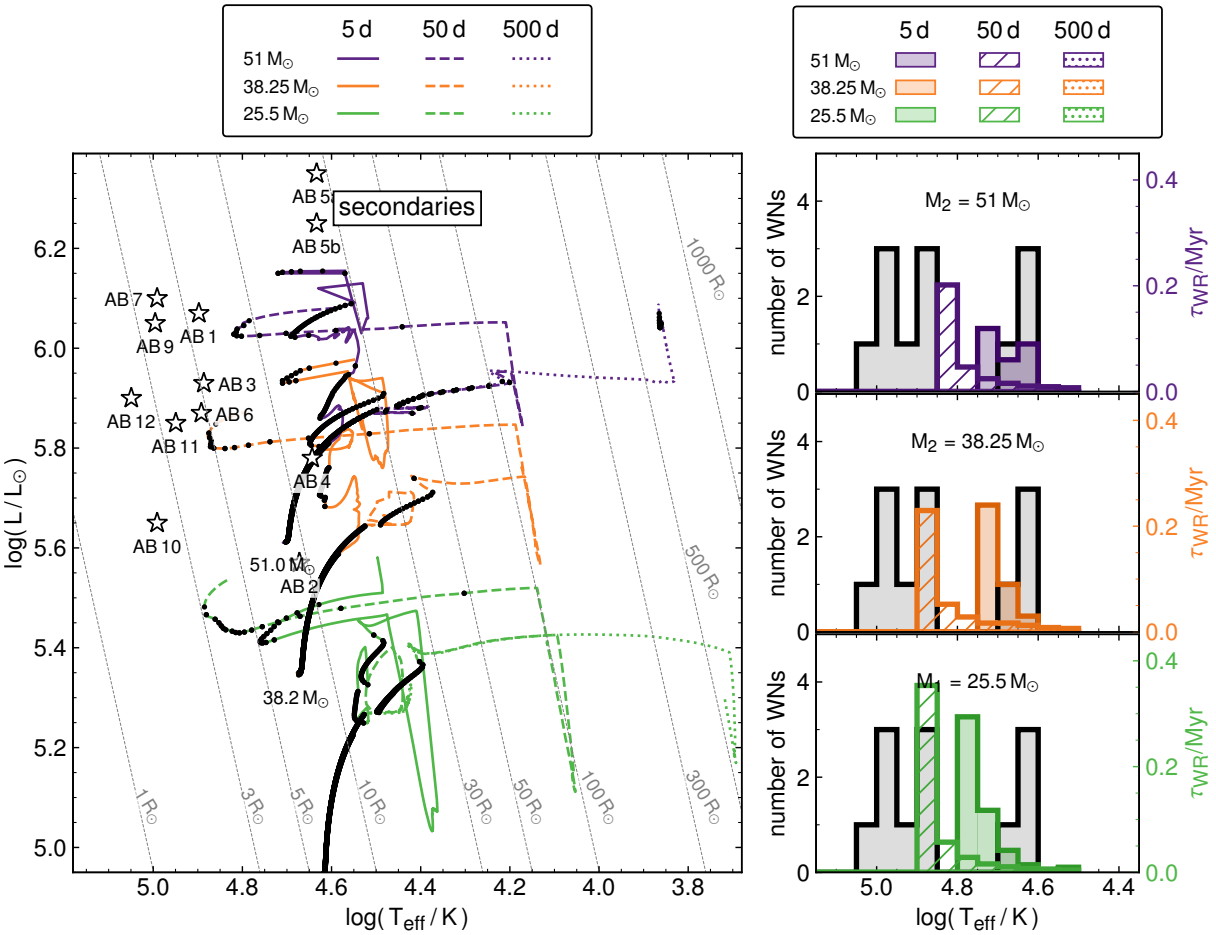

Figure 2: Same as Fig. 1, but now showing the tracks and the histograms of the secondaries. Note, that they have been calculated with a fixed mass ratio of $q = 0.85$.

the star can accrete mostly conservatively and gets rejuvenated. In systems with longer orbital periods (here, $P_{\rm ini} \gtrsim 50\,$d), the secondary only accretes a few percent of its initial mass before it reaches critical rotation, preventing further accretion onto the star.

The secondaries in the systems with initially short orbital periods ($P_{\rm ini} = 5\,$d; solid lines in Fig. 2), undergo almost fully conservative mass transfer and can accrete more than $10\,M_\odot$. Consequently, they get rejuvenated, which can be seen by a jump in luminosity. Due to the presence of a stabilizing chemical gradient between the currently hydrogen-burning core and the envelope, the core grows less than the envelope in response to the accretion. This leads to a quick steepening of the chemical gradient between the core and the envelope and alters the structure of the envelope, causing the formation of an intermediate convection zone while still on the main sequence. These fundamental structural changes cause the secondary to respond differently to mass loss during the mass-transfer phase onto its black hole companion. As a result, the star retains an extended hydrogen envelope with surface hydrogen abundances around 0.4. This leads to moderate effective temperatures of about 50 kK. These systems can explain well the observed properties of SMC AB 2 and SMC AB 4.

The secondaries in the systems with initially long orbital periods ($P_{\rm ini} = 50\,$d and $500\,$d;

dashed and dotted lines in Fig. 2) quickly spin up due to the accretion of material and reach their critical rotation, leading to slightly lower surface temperatures. Since in our models there is no mechanism slowing the secondaries down efficiently, they cannot accrete much material and thus, do not get rejuvenated. As a result, the secondary responds to mass loss during the later mass transfer onto the compact companion in the same way as a primary star (e.g., the evolutionary tracks of the primaries presented in Fig. 1 look surprisingly similar to those of the non-conservative accretors shown as dashed and dotted lines in Fig. 2). This means that the non-rejuvenated secondaries evolve into hydrogen-poor WN-type stars with temperatures around 100 kK.

According to the model calculations, the observed properties of the WR stars SMC AB 2 and SMC AB 4 ($T \approx 50$ kK, $\log(L/L_{\odot}) < 5.8$) can only be explained if these stars were originally secondaries that got rejuvenated during an efficient mass-transfer phase and should have a (so far undetected) compact companion. To make this theory testable, I studied the binary evolution models to determine if there is an observational property, that allows us to distinguish between WN-type stars that once were rejuvenated or that are just in a short transition phase or suffer from inflated envelopes due to their proximity to the Eddington limit. In Fig. 3 the stellar evolution tracks of the primary stars and the secondaries are color-coded by their surface oxygen abundance. The primary stars (top panel of Fig. 3), and the non-rejuvenated secondaries (dashed and dotted lines in the bottom panel of Fig. 3) efficiently strip off their hydrogen-rich envelopes, exposing the former hydrogen-burning core and have surface oxygen abundances consistent with the CNO equilibrium abundance ($X_{\rm O} = 2 \times 10^{-5}$). The rejuvenated secondaries (solid lines in the lower panel of Fig. 3), however, do not lose their entire hydrogen envelope during mass transfer and only expose layers that were on top of the former hydrogen-burning core. This is reflected in about one order of magnitude higher surface oxygen abundances ($X_{\rm O} \approx 20 \times 10^{-5}$) than the CNO equilibrium value. This difference in the surface oxygen abundance should be detectable and measurable in the spectra of WN-type stars, allowing us to gain new insights into their previous evolutionary history.

Unfortunately, in previous spectral analyses of WN-type stars in the SMC, surface oxygen abundance has rarely been studied, due to the lack of measurable oxygen lines – which are not strongly affected by stellar winds or X-rays – in the available optical and (far-)UV spectra. For the WN stars with moderate temperatures, O IV is expected to be the dominant ion in the wind. In the UV spectrum, oxygen lines are often blended with iron lines, making them difficult to distinguish. However, in the optical range, there are multiple O IV lines around $\lambda\lambda$ 3381 – 3483 Å, which were not previously covered or included in WR star analyses. With modern optical spectrographs such as X-Shooter, this wavelength range is now included by default. Fortunately, SMC AB 4, one of the WN-type stars in the SMC with a moderate temperature, has an archival X-Shooter spectrum that offers both high resolution and a high signal-to-noise ratio. Using the previously calculated stellar atmosphere model for SMC AB 4 from Hainich et al. (2015) as a basis, I calculated two new stellar atmosphere models with PoWR (Gräfener et al., 2002; Hamann and Gräfener, 2003; Hamann and Gräfener, 2004; Todt et al., 2015; Sander et al., 2015) which incorporate oxygen abundances of $X_{\rm O} = 2 \times 10^{-5}$ and $X_{\rm O} = 20 \times 10^{-5}$. Figure 4 shows the observed and synthetic spectra across the full spectral range covered by the UBV arm

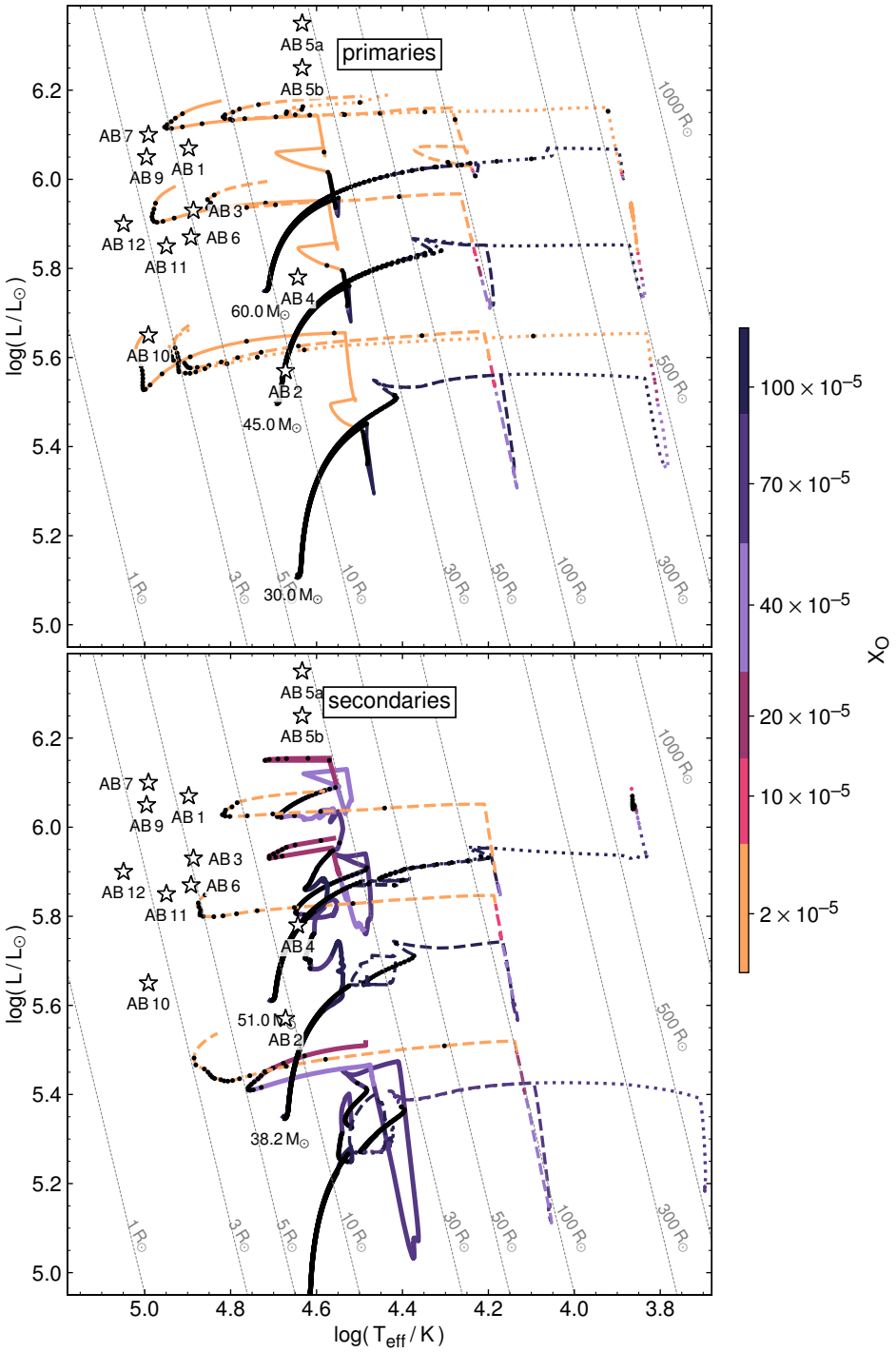

Figure 3: (*Top*) HRD showing the stellar evolution tracks of the primaries of the binary evolution grid. The tracks are labeled by their initial mass. Solid, dashed, and dotted lines correspond to initial orbital periods of 5 d, 50 d, and 500 d, respectively. The tracks are overplotted by black dots representing equidistant timesteps of $\Delta t = 30\,000$ yr and, thus, highlighting well-populated regions. Furthermore, the tracks are color-coded according to the surface oxygen abundance of a stellar model. (*Bottom*) Same as the top panel, but now for the secondaries of the model grid.

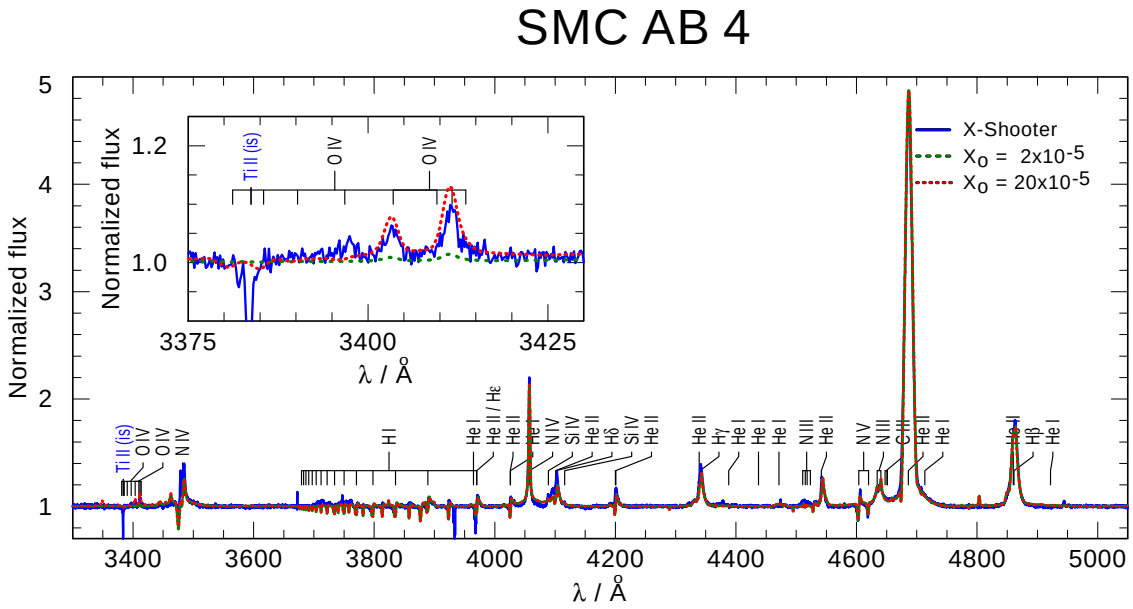

Figure 4: Observed (blue solid line) and synthetic (dotted green and red lines) optical spectrum of the WN-star SMC AB 4. The inset shows a zoomed-in view of the O IV multiplet. The stellar atmosphere models are calculated with oxygen abundances of $X_{\rm O} = 2 \times 10^{-5}$ and $X_{\rm O} = 20 \times 10^{-5}$, and are shown as green dotted and red dotted lines, respectively. Only the model with the higher surface oxygen abundance agrees with the observations.

of X-Shooter, along with a zoomed-in view of the O IV lines. A comparison of the synthetic model spectra with the observed spectrum reveals that the model with the higher surface oxygen abundance fits the observed data better than the one with the CNO equilibrium abundance. According to the binary evolution models predictions, this implies that SMC AB 4 must have been a secondary star in a binary system and has a so far unseen compact companion.

4. Summary

The observed population of WR stars in the SMC includes 12 WN-type stars. This low-metallicity population is expected to be minimally influenced by metallicity-dependent effects, such as envelope inflation, which typically positions stars at cooler temperatures. Despite this, the population exhibits an unexpected bimodal temperature distribution. While most WN-type stars reside at high temperatures of about 100 kK, a few exceptions with moderate temperatures of about 50 kK exist, which so far cannot be explained by stellar evolution models.

In this work, I presented a small grid of state-of-the-art binary evolution models that follow the evolution of both the primary and secondary stars in detail. The analysis of these models leads to the following hypothesis on the temperature distribution of low-metallicity WR populations: hot, hydrogen-poor WN-type stars are formed either from primary stars or from secondaries that have accreted less than a few percent of their initial mass and did not get rejuvenated. WN stars with moderate temperatures originate from two possible channels. Either they

are former accretors that have been rejuvenated, consequently altering their internal structure and leading to surface oxygen abundances above the CNO equilibrium value ($X_{\rm O} = 20 \times 10^{-5}$), or, in the case of more luminous stars ($\log(L/L_{\odot}) \gtrsim 6.1$), they are extended sources affected by envelope inflation, but maintain surface oxygen abundances consistent with the CNO equilibrium ($X_{\rm O} = 2 \times 10^{-5}$). This implies that all low-metallicity WN-type stars with moderate temperatures and luminosities below $\log(L/L_{\odot}) \lesssim 6.1$ should harbor a compact object as a companion.

The first observational support for this hypothesis comes from the system SMC AB 4 which exhibits the predicted higher surface oxygen abundance. However, this system does not show signs of binarity so far, questioning if it is accompanied by an unseen compact companion that could have circumvented detection. Further large-scale observational campaigns, focusing on the surface oxygen abundances of WN-type stars and their multiplicity properties, are needed to advance our understanding of massive binary evolution and its impact on the stellar properties of WR populations.

Acknowledgments

DP acknowledges financial support by the Deutsches Zentrum für Luft- und Raumfahrt (DLR) grant FKZ 50OR2005.

Further Information

Author's ORCID identifier

0000-0002-5453-2788 (Daniel PAULI)

Conflicts of interest

The author declares that there is no conflict of interest.

References

Aguilera-Dena, D. R., Langer, N., Antoniadis, J., and Müller, B. (2020) Precollapse properties of superluminous supernovae and long gamma-ray burst progenitor model. *ApJ*, **901**(2), 114. https://doi.org/10.3847/1538-4357/abb138.

Aguilera-Dena, D. R., Langer, N., Antoniadis, J., Pauli, D., Dessart, L., Vigna-Gómez, A., Gräfener, G., and Yoon, S.-C. (2022) Stripped-envelope stars in different metallicity environments. I. Evolutionary phases, classification, and populations. *A&A*, **661**, A60. https://doi.org/10.1051/0004-6361/202142895.

Asplund, M., Grevesse, N., Sauval, A. J., and Scott, P. (2009) The chemical composition of the Sun. *ARA&A*, **47**, 481–522. https://doi.org/10.1146/annurev.astro.46.060407.145222.

Böhm-Vitense, E. (1958) Über die Wasserstoffkonvektionszone in Sternen verschiedener Effektivtemperaturen und Leuchtkräfte. *ZAp*, **46**, 108–143. https://ui.adsabs.harvard.edu/abs/1958ZA.....46..108B.

Brott, I., de Mink, S. E., Cantiello, M., Langer, N., de Koter, A., Evans, C. J., Hunter, I., Trundle, C., and Vink, J. S. (2011) Rotating massive main-sequence stars: I. Grids of evolutionary models and isochrones. *A&A*, **530**, A115. https://doi.org/10.1051/0004-6361/201016113.

Castor, J. I., Abbott, D. C., and Klein, R. I. (1975) Radiation-driven winds in Of stars. *ApJ*, **195**(1), 157–174. https://doi.org/10.1086/153315.

Conti, P. S. (1976) On the relationship between Of and WR stars. *MSRSL*, **9**, 193–212.

Crowther, P. A. (2007) Physical properties of Wolf–Rayet stars. *ARA&A*, **45**, 177–219. https://doi.org/10.1146/annurev.astro.45.051806.110615.

Dessart, L., Hillier, D. J., Livne, E., Yoon, S.-C., Woosley, S., Waldman, R., and Langer, N. (2011) Core-collapse explosions of Wolf–Rayet stars and the connection to Type IIb/Ib/Ic supernovae. *MNRAS*, **414**(4), 2985–3005. https://doi.org/10.1111/j.1365-2966.2011.18598.x.

Dray, L. M., Tout, C. A., Karakas, A. I., and Lattanzio, J. C. (2003) Chemical enrichment by Wolf–Rayet and asymptotic giant branch stars. *MNRAS*, **338**(4), 973–989. https://doi.org/10.1046/j.1365-8711.2003.06142.x.

Gräfener, G., Koesterke, L., and Hamann, W.-R. (2002) Line-blanketed model atmospheres for WR stars. *A&A*, **387**(1), 244–257. https://doi.org/10.1051/0004-6361:20020269.

Gräfener, G., Owocki, S. P., and Vink, J. S. (2012) Stellar envelope inflation near the Eddington limit. ımplications for the radii of Wolf–Rayet stars and luminous blue variables. *A&A*, **538**, A40. https://doi.org/10.1051/0004-6361/201117497.

Groh, J. H., Meynet, G., and Ekström, S. (2013) Massive star evolution: luminous blue variables as unexpected supernova progenitors. *A&A*, **550**, L7. https://doi.org/10.1051/0004-6361/201220741.

Hainich, R., Pasemann, D., Todt, H., Shenar, T., Sander, A., and Hamann, W.-R. (2015) Wolf–Rayet stars in the Small Magellanic Cloud. I. Analysis of the single WN stars. *A&A*, **581**, A21. https://doi.org/10.1051/0004-6361/201526241.

Hamann, W.-R. and Gräfener, G. (2003) A temperature correction method for expanding atmospheres. *A&A*, **410**(3), 993–1000. https://doi.org/10.1051/0004-6361:20031308.

Hamann, W.-R. and Gräfener, G. (2004) Grids of model spectra for WN stars, ready for use. *A&A*, **427**(2), 697–704. https://doi.org/10.1051/0004-6361:20040506.

Heger, A., Langer, N., and Woosley, S. E. (2000) Presupernova evolution of rotating massive stars. I. Numerical method and evolution of the internal stellar structure. *ApJ*, **528**(1), 368–396. https://doi.org/10.1086/308158.

Hunter, I., Dufton, P. L., Smartt, S. J., Ryans, R. S. I., Evans, C. J., Lennon, D. J., Trundle, C., Hubeny, I., and Lanz, T. (2007) The VLT-FLAMES survey of massive stars: surface chemical compositions of B-type stars in the Magellanic Clouds. *A&A*, **466**(1), 277–300. https://doi.org/10.1051/0004-6361:20066148.

Hurley, J. R., Tout, C. A., and Pols, O. R. (2002) Evolution of binary stars and the effect of tides on binary populations. *MNRAS*, **329**(4), 897–928. https://doi.org/10.1046/j.1365-8711.2002.05038.x.

Inserra, C., Smartt, S. J., Jerkstrand, A., Valenti, S., Fraser, M., Wright, D., Smith, K., Chen, T.-W., Kotak, R., Pastorello, A., Nicholl, M., Bresolin, F., Kudritzki, R. P., Benetti, S., Botticella, M. T., Burgett, W. S., Chambers, K. C., Ergon, M., Flewelling, H., Fynbo, J. P. U., Geier, S., Hodapp, K. W., Howell, D. A., Huber, M., Kaiser, N., Leloudas, G., Magill, L., Magnier, E. A., McCrum, M. G., Metcalfe, N., Price, P. A., Rest, A., Sollerman, J., Sweeney, W., Taddia, F., Taubenberger, S., Tonry, J. L., Wainscoat, R. J., Waters, C., and Young, D. (2013) Super-Luminous Type Ic supernovae: Catching a magnetar by the tail. *ApJ*, **770**(2), 128. https://doi.org/10.1088/0004-637X/770/2/128.

Kippenhahn, R., Ruschenplatt, G., and Thomas, H.-C. (1980) The time scale of thermohaline mixing in stars. *A&A*, **91**(1-2), 175–180. https://ui.adsabs.harvard.edu/abs/1980A&A....91..175K.

Koenigsberger, G., Morrell, N., Hillier, D. J., Gamen, R., Schneider, F. R. N., González-Jiménez, N., Langer, N., and Barbá, R. (2014) The HD 5980 multiple system: Masses and evolutionary status. *AJ*, **148**(4), 62. https://doi.org/10.1088/0004-6256/148/4/62.

Kurt, C. M. and Dufour, R. J. (1998) The chemical composition of H II regions in the Magellanic Clouds: New calculations using modern atomic data. In *The sixth Texas–Mexico conference on astrophysics: astrophysical plasmas – near and far*, edited by Dufour, R. J. and Torres-Peimbert, S., *RMxAA Conference Series*, volume 7, pages 202–206. https://ui.adsabs.harvard.edu/abs/1998RMxAC...7..202K.

Langer, N., Fricke, K. J., and Sugimoto, D. (1983) Semiconvective diffusion and energy transport. *A&A*, **126**(1), 207–208. https://ui.adsabs.harvard.edu/abs/1983A&A...126..207L.

Maeder, A. (1983) Evolution of chemical abundances in massive stars. I. OB stars, Hubble–Sandage variables and Wolf–Rayet stars. Changes at stellar surfaces and galactic enrichment by stellar winds. *A&A*, **120**, 113–129. https://ui.adsabs.harvard.edu/abs/1983A&A...120..113M.

Nieuwenhuijzen, H. and de Jager, C. (1990) Parametrization of stellar rates of mass loss as functions of the fundamental stellar parameters M, L, and R. *A&A*, **231**, 134–136. https://ui.adsabs.harvard.edu/abs/1990A&A...231..134N.

Paczyński, B. (1967) Evolution of close binaries. V. The evolution of massive binaries and the formation of the Wolf–Rayet stars. *AcA*, **17**(4), 355–380. https://ui.adsabs.harvard.edu/abs/1967AcA....17..355P.

Paxton, B., Bildsten, L., Dotter, A., Herwig, F., Lesaffre, P., and Timmes, F. (2011) Modules for Experiments in Stellar Astrophysics (MESA). *ApJS*, **192**(1), 3. https://doi.org/10.1088/0067-0049/192/1/3.

Paxton, B., Cantiello, M., Arras, P., Bildsten, L., Brown, E. F., Dotter, A., Mankovich, C., Montgomery, M. H., Stello, D., Timmes, F. X., and Townsend, R. (2013) Modules for Experiments in Stellar Astrophysics (MESA): Planets, oscillations, rotation, and massive stars. *ApJS*, **208**(1), 4. https://doi.org/10.1088/0067-0049/208/1/4.

Paxton, B., Marchant, P., Schwab, J., Bauer, E. B., Bildsten, L., Cantiello, M., Dessart, L., Farmer, R., Hu, H., Langer, N., Townsend, R. H. D., Townsley, D. M., and Timmes, F. X. (2015) Modules for Experiments in Stellar Astrophysics (MESA): Binaries, pulsations, and explosions. *ApJS*, **220**(1), 15. https://doi.org/10.1088/0067-0049/220/1/15.

Paxton, B., Schwab, J., Bauer, E. B., Bildsten, L., Blinnikov, S., Duffell, P., Farmer, R., Goldberg, J. A., Marchant, P., Sorokina, E., Thoul, A., Townsend, R. H. D., and Timmes, F. X. (2018) Modules for Experiments in Stellar Astrophysics (MESA): Convective boundaries, element diffusion, and massive star explosions. *ApJS*, **234**(2), 34. https://doi.org/10.3847/1538-4365/aaa5a8.

Paxton, B., Smolec, R., Schwab, J., Gautschy, A., Bildsten, L., Cantiello, M., Dotter, A., Farmer, R., Goldberg, J. A., Jermyn, A. S., Kanbur, S. M., Marchant, P., Thoul, A., Townsend, R. H. D., Wolf, W. M., Zhang, M., and Timmes, F. X. (2019) Modules for Experiments in Stellar Astrophysics (MESA): Pulsating variable stars, rotation, convective boundaries, and energy conservation. *ApJS*, **243**(1), 10. https://doi.org/10.3847/1538-4365/ab2241.

Sander, A., Shenar, T., Hainich, R., Gímenez-García, A., Todt, H., and Hamann, W.-R. (2015) On the consistent treatment of the quasi-hydrostatic layers in hot star atmospheres. *A&A*, **577**, A13. https://doi.org/10.1051/0004-6361/201425356.

Sanyal, D., Grassitelli, L., Langer, N., and Bestenlehner, J. M. (2015) Massive main-sequence stars evolving at the Eddington limit. *A&A*, **580**, A20. https://doi.org/10.1051/0004-6361/201525945.

Schootemeijer, A., Langer, N., Grin, N. J., and Wang, C. (2019) Constraining mixing in massive stars in the Small Magellanic Cloud. *A&A*, **625**, A132. https://doi.org/10.1051/0004-6361/201935046.

Shenar, T., Hainich, R., Todt, H., Moffat, A. F. J., Sander, A., Oskinova, L. M., Ramachandran, V., Munoz, M., Pablo, H., Sana, H., and Hamann, W.-R. (2018) The shortest-period Wolf–Rayet binary in the Small Magellanic Cloud: Part of a high-order multiple system. Spectral and orbital analysis of SMC AB 6. *A&A*, **616**, A103. https://doi.org/10.1051/0004-6361/201833006.

Shenar, T., Hainich, R., Todt, H., Sander, A., Hamann, W.-R., Moffat, A. F. J., Eldridge, J. J., Pablo, H., Oskinova, L. M., and Richardson, N. D. (2016) Wolf–Rayet stars in the Small

Magellanic Cloud. II. Analysis of the binaries. *A&A*, **591**, A22. https://doi.org/10.1051/0004-6361/201527916.

Shenar, T., Sablowski, D. P., Hainich, R., Todt, H., Moffat, A. F. J., Oskinova, L. M., Ramachandran, V., Sana, H., Sander, A. A. C., Schnurr, O., St-Louis, N., Vanbeveren, D., Götberg, Y., and Hamann, W.-R. (2019) The Wolf–Rayet binaries of the nitrogen sequence in the Large Magellanic Cloud. Spectroscopy, orbital analysis, formation, and evolution. *A&A*, **627**, A151. https://doi.org/10.1051/0004-6361/201935684.

Shenar, T., Sablowski, D. P., Hainich, R., Todt, H., Moffat, A. F. J., Oskinova, L. M., Ramachandran, V., Sana, H., Sander, A. A. C., Schnurr, O., St-Louis, N., Vanbeveren, D., Götberg, Y., and Hamann, W.-R. (2020) The Wolf–Rayet binaries of the nitrogen sequence in the Large Magellanic Cloud. Spectroscopy, orbital analysis, formation, and evolution (Corrigendum). *A&A*, **641**, C2. https://doi.org/10.1051/0004-6361/201935684e.

Spruit, H. C. (2002) Dynamo action by differential rotation in a stably stratified stellar interior. *A&A*, **381**(3), 923–932. https://doi.org/10.1051/0004-6361:20011465.

Todt, H., Kniazev, A. Y., Gvaramadze, V. V., Hamann, W.-R., Pena, M., Graefener, G., Buckley, D., Crause, L., Crawford, S. M., Gulbis, A. A. S., Hettlage, C., Hooper, E., Husser, T.-O., Kotze, P., Loaring, N., Nordsieck, K. H., O'Donoghue, D., Pickering, T., Potter, S., Romero-Colmenero, E., Vaisanen, P., Williams, T., and Wolf, M. (2015) Hydrogen–deficient central stars of planetary nebulae. In *19th European Workshop on White Dwarfs*, edited by Dufour, P., Bergeron, P., and Fontaine, G., *Astronomical Society of the Pacific Conference Series*, volume 493, pages 539–543. https://www.aspbooks.org/a/volumes/article_details/?paper_id=37042.

Trundle, C., Dufton, P. L., Hunter, I., Evans, C. J., Lennon, D. J., Smartt, S. J., and Ryans, R. S. I. (2007) The VLT-FLAMES survey of massive stars: evolution of surface N abundances and effective temperature scales in the Galaxy and Magellanic Clouds. *A&A*, **471**(2), 625–643. https://doi.org/10.1051/0004-6361:20077838.

Venn, K. A. (1999) A-Type supergiant abundances in the Small Magellanic Cloud: Probes of evolution. *ApJ*, **518**(1), 405–421. https://doi.org/10.1086/307278.

Vink, J. S., de Koter, A., and Lamers, H. J. G. L. M. (2001) Mass-loss predictions for O and B stars as a function of metallicity. *A&A*, **369**(2), 574–588. https://doi.org/10.1051/0004-6361:20010127.

Weaver, R., McCray, R., Castor, J., Shapiro, P., and Moore, R. (1977) Interstellar bubbles. II. Structure and evolution. *ApJ*, **218**, 377–395. https://doi.org/10.1086/155692.